

# Molecular Modeling of Single Beta-Sheet and the Beta-Sheet Stack of Amyloid Beta Protein 25 – 35

Vita Duka, *University of Latvia*, Isabella Bestel, *Victor Segalen University of Bordeaux II*,  
Cezary Czaplowski, *University of Gdansk*, Adam Liwo, *University of Gdansk*,  
Inta Liepina, *Latvian Institute of Organic Synthesis*

**Abstract.** Amyloidosis is the misfolding of soluble proteins followed by their self-assembling, resulting in aggregation into insoluble fibrils which replace the functional cells or block the connectivity between the cells. The mechanism of amyloid formation is still unclear. The amyloid beta protein 1-42 is responsible for formation of human amyloidosis leading to Alzheimer disease. In the present work we studied the formation of amyloid  $\beta$ -structure of the amyloid beta protein fragment 25-35 (Abeta 25-35), GSNKGAIIGLM. A flat, parallel single six stranded beta-sheet (6Abeta 25-35) and ten stranded beta-sheet (10Abeta 25-35), as well as a stack built from six stranded beta-sheet (6x6Abeta 25-35) were simulated by molecular dynamics (MD) for 210 ns, 310 ns and 76 ns, respectively, using Amber 9.0 program package, f99 force field. Temperature was increased stepwise from 10K with the constant temperature platos at 200K and at 309 K.

6Abeta 25-35 and 10Abeta 25-35 single beta sheet systems show the stable  $\beta$ -structure at 200K temperature, but collapse losing  $\beta$ -structure at 309K temperature, indicating that supplementary  $\beta$ -sheets are required for  $\beta$ -structure stabilization. The additional four strands in 10Abeta 25-35 comparing to 6Abeta 25-35 do not stabilize the  $\beta$ -sheet.

In the 6x6Abeta 25-35 beta-sheet stack the strongest intra  $\beta$ -sheet interactions, which keeps the stack together, is comprised by Ile31 and Ile32 forming the main part of the hydrophobic core. Apart from that, in the  $\beta$ -sheet stack the  $\beta$ -sheets are kept together by Leu34 and Met35 hydrophobic interactions and Ser26 and Asn27 electrostatic interactions. In several cases the sidechain of Lys28 makes hydrogen bonds with the backbone carbonyl of Gly29 in the nearby  $\beta$ -sheet. The C-terminal part of the  $\beta$ -sheet stack is more prone to keep the  $\beta$ -sheet structure while the N-terminal part of the  $\beta$ -sheet stack is more flexible which is in accord with the experimental data [39]. A single strand of the Abeta 25-35 stack tends to jump away from the stack and turns from  $\beta$ -structure to coil conformation with the further perspective to turn to  $\alpha$ -helix. This is in accordance with literature data suggesting that the Abeta 25-35 peptide could form both  $\beta$ -structure and  $\alpha$ -helical structure in water and membrane environment depending on conditions [38].

**Keyword:** Amyloid beta protein, Abeta, amyloidosis, molecular dynamics, beta-sheet.

## I. INTRODUCTION

Proteins fold into native three-dimensional structure to perform the biological functions. Under specific conditions, such as pH lowering, temperature elevation, mutations, oxidation, proteins unfold, and can subsequently be misfolded [1].

Amyloids are insoluble and fibrous proteins which arise after unfolding and misfolding of soluble proteins. Abnormal accumulation of amyloids in organs may lead to amyloidosis. Amyloidosis is extracellular protein deposits that form fibrils either in the brain or other organs [2, 3]. Amyloid fibrils are responsible for several neurodegenerative diseases including Alzheimer's, Parkinson's, and Huntington's diseases [4, 5], and such conformational diseases as type 2 diabetes, and Finnish familial amyloidosis. The different proteins and peptides neither related in sequence or length, nor sharing sequence homology can form amyloid fibrils, exhibit similar insoluble filaments and fibrillation responses [2, 6, 7], and the fibrils from different proteins have similar fibril structures. The mechanism of amyloid formation is still unclear [8].

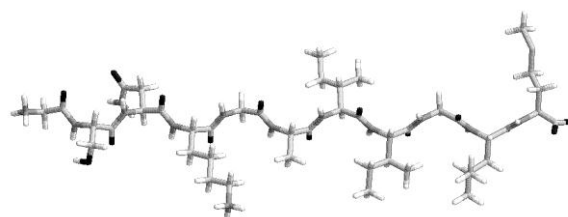


Fig. 1. Amyloid beta peptide fragment 25-35 (Abeta 25-35, GSNKGAIIGLM).

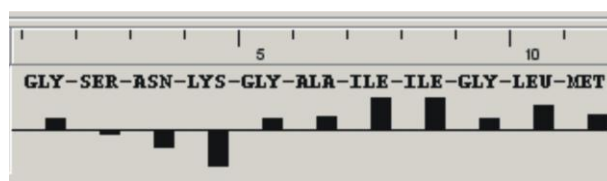


Fig. 2. Hydrophobicity of Abeta 25-36 (calculated by MOE [40]).

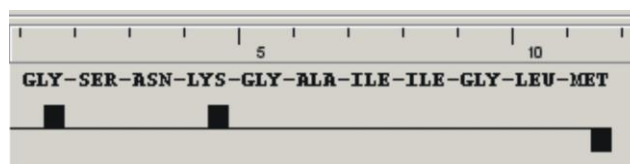


Fig. 3. The Abeta 25-35 peptide charge, calculated by MOE [39].

Alzheimer's disease (AD) is characterized by accumulation of Amyloid beta (Abeta) plaques outside and around nerve cells in the brain region known to be important for intellectual functions [9, 10].

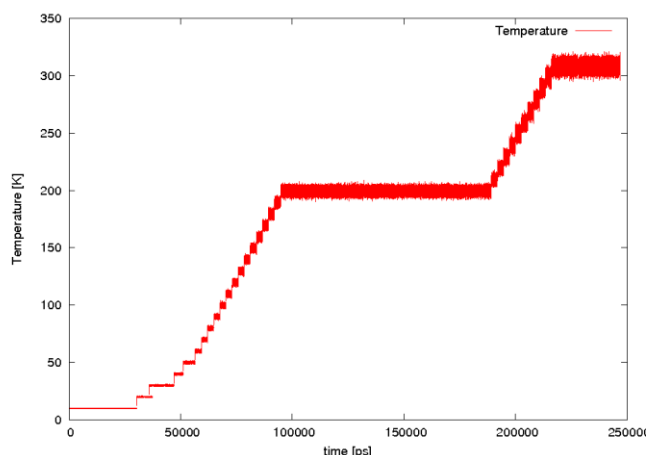


Fig. 4. Temperature protocol of both 6Abeta25-35 and 10Abeta 25-35 systems.

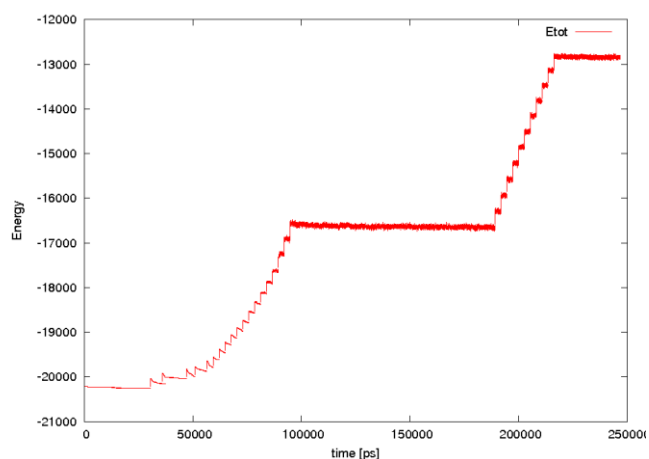


Fig. 5. Energy over time of the 6Abeta 25-35 system.

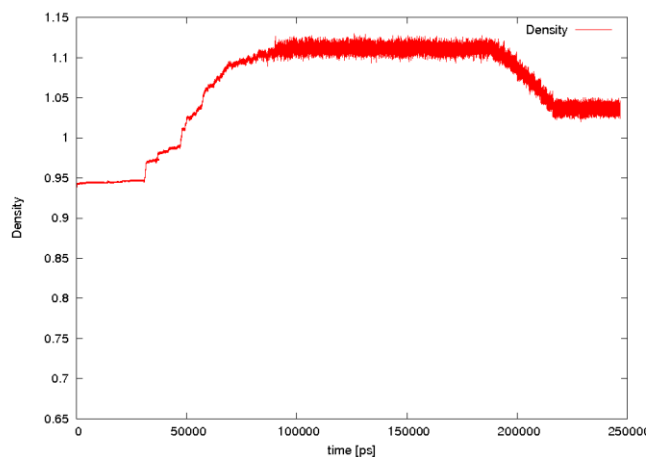


Fig. 6. Density over time of the 6Abeta 25-35 system.

Abeta protein is cleaved from Amyloid Precursor Protein (APP), a transmembrane glycoprotein, subsequently by beta and gamma secretases, thus creating Abeta 1-40 or Abeta 1-42. Abeta 1-42 is more prone to aggregate into fibrils, and it is the major component of amyloid plaques [11]. Abeta 1-42

is found in cerebrovascular plaques and in neuritic plaques, which cause neurodegeneration and subsequent loss of memory in Alzheimer's disease.

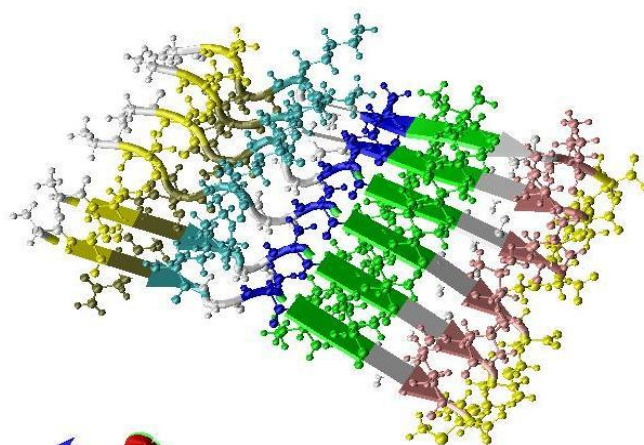


Fig. 7. Front view of 6Abeta 25-35 system after 30ns of MD.

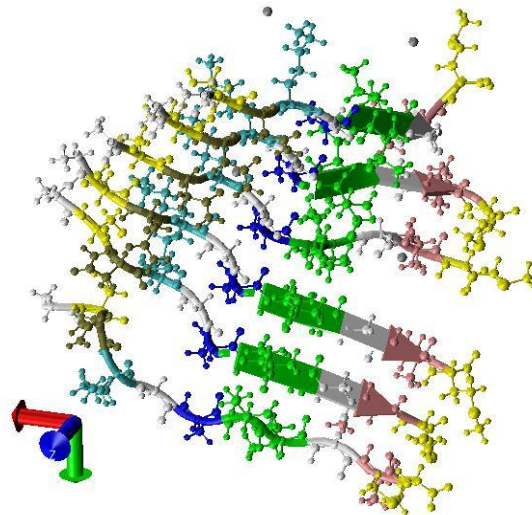


Fig. 8. Front view of 6Abeta 25-35 system after 145ns of MD.

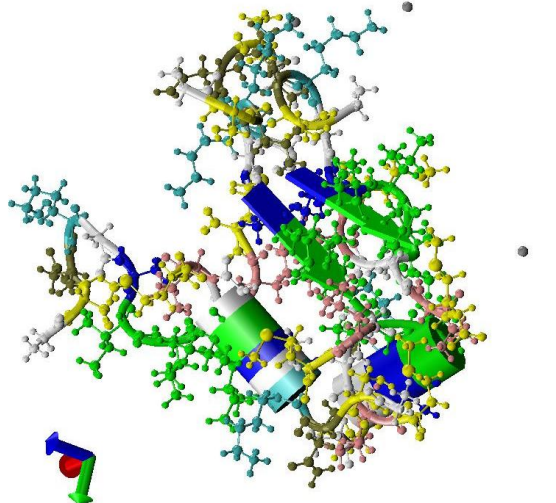


Fig. 9. Front view of 6Abeta 25-35 system with water after 310ns of MD run

In the plasma and cerebrospinal fluid Abeta is a normal amyloid precursor protein metabolism product, soluble peptide of 40 or 42 amino acid residues [12, 13]. Amyloid fibril formation results directly from unfolding of Abeta peptide native conformation and subsequent misfolding [14].

Insoluble fibrils form as a result of aggregation of Abeta peptides [12], and it is believed that because of fibrillogenic nature Amyloid-beta peptide is causative agent in the etiology of Alzheimer's disease.

Interacting with membrane Abeta oligomers and protofibrils may be the cause of neurotoxicity [15, 16, 17] and subsequent cell degeneration and apoptoses. Amyloid-beta peptide neurotoxicity is related to interactions of the Amyloid-beta peptide and the membrane, and the pore formation [18, 19], and membrane disruption. The formation of amyloid plaques correlates with any conformational disease, but whether fibrils themselves, misfolded oligomers, or other factors are the causal agents of diseases remains unclear [20 - 22]. The pore action mechanism in the neurodegenerative process has not been established yet [23].

Abeta 25-35 is a the biologically active region of Abeta 1-42 protein, the shortest fragment which possesses amyloidogenic, neurotoxic and channel forming abilities similar to that of Abeta 1-42 [24 - 29].

Abeta 25-35 and its analogues insert themselves into the membrane hydrophobic region using the C-terminal or central hydrophobic residues [23]. Abeta 25-35 enter the membrane's hydrophobic core, by the formation of continuous helical structures of its C-terminal residues [23].

Nevertheless, experiments on membranes show, that mutations in N-terminal region N27A-Abeta(25-35) result in a lower degree of aggregation and a lower neurotoxicity, and mutations in C-terminal M35A-Abeta(25-35) result to the peptide more prone to aggregation with a higher neurotoxicity, suggesting that the neurotoxicity of these Abeta(25-35) analogs cannot be characterized by their hydrophobicities alone [23].

The present work by means of molecular dynamics (MD) studied the formation of amyloid  $\beta$ -structure of the amyloid beta protein fragment 25-35 (**Abeta 25-35**):

**Gly25-Ser26-Asn27-Lys28-Gly29-Ala30-Ile31-Ile32-Gly33-Leu34-Met35.**

Abeta peptide 10-42 consists of hydrophobic C-terminal domain residues (29-42) that adopts beta-strand conformation and an N-terminal domain 10-24 whose sequence permits the existence of a dynamical equilibrium between an alpha-helix and a beta-strand [30]. Similarly, Abeta(25-35) consists of hydrophobic C-terminal domain residues (29-35) and hydrophilic N-terminal part 25-28 (Fig. 2 –Fig. 3).

We chose the parallel beta sheet for Abeta 25-35 peptide for molecular dynamics simulations, since NMR measurements suggest that the peptide beta amyloid (10–35) has a parallel  $\beta$ -sheet structure, and that the peptide adopts the structure of an extended parallel beta-sheet in-register at pH 7.4 [31], and there is no evidence for a turn to be found in the putative turn region comprising residues 25-29, Gly25-Ser26-Asn27-Lys28-

Gly29 [31]. The parallel  $\beta$ -sheet structure for amyloid beta peptide is confirmed also by D'Ursi and Antzutkin [32, 36].

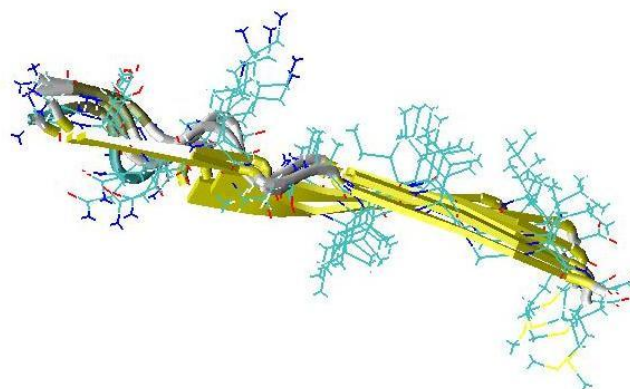


Fig. 10. Side view of 6Abeta 25-35 system after 30ns of MD run.

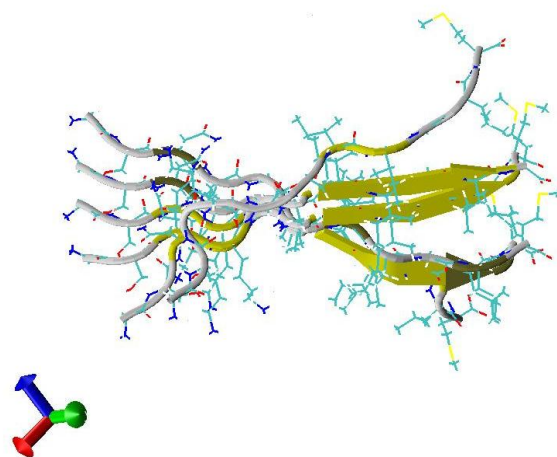


Fig. 11. Side view of 6Abeta 25-35 system after 145ns of MD run.

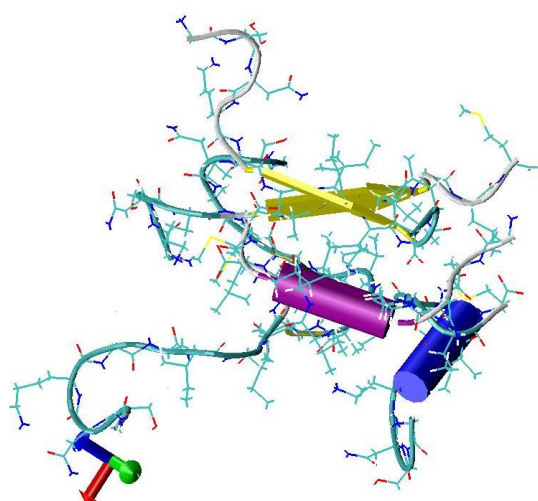


Fig. 12. Side view of 6Abeta 25-35 system with water after 310ns of MD run.

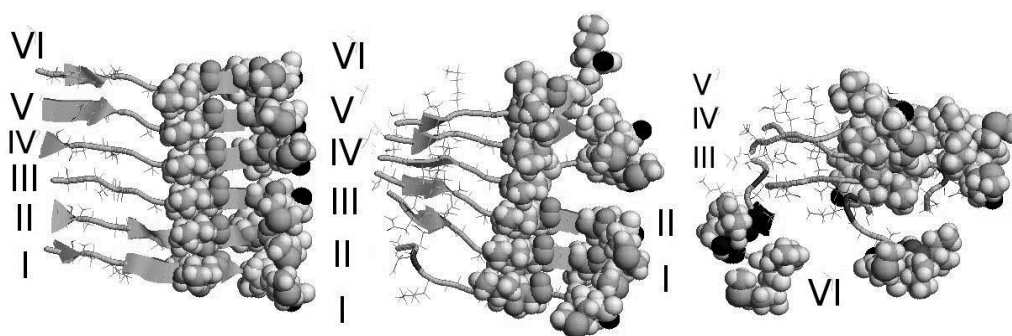


Fig. 13. Hydrophobic residues Ile, Leu, Met (spacefill) keeping together the 6Abeta 25-35 system. Snapshots at a) 30 ns, b) 145 ns and c) 256 ns of MD run

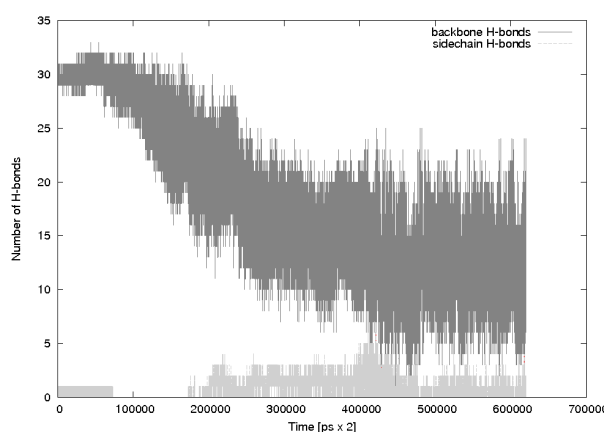


Fig. 14. Hydrogen bonding of 6Abeta 25-35 system  $\beta$ -sheet. Number of backbone hydrogen bonds – dark gray, number of sidechain hydrogen bonds – light gray.

## II. METHODS

A flat, parallel single six stranded beta-sheet (**6Abeta 25-35**) and ten stranded beta-sheet (**10Abeta 25-35**) of Abeta 25-35 were constructed using the peptide Abeta 25-35 strand. The parallel beta strand composition was chosen because the fibrils composed of the full-length Abeta 1-40 peptide or shorter peptide sequences were found to fold into a parallel beta-sheet structure [31, 32].

Both systems 6Abeta 25-35 and 10Abeta 25-35 were surrounded by chlorine counterions to neutralize the net charge and by a 5 Å layer of explicit water molecules. The 6Abeta 25-35 and 10Abeta 25-35 systems consisting of 5361 atoms (930 solute atoms) and 8022 atoms (1550 solute atoms) respectively, were minimized and subjected to molecular dynamics (MD) by using the Amber 9.0 program package [33-35], with the f99 force field, periodic water box, and NTP protocol (constant number of particles, temperature, pressure).

The starting temperature was 10 K for both systems, then the temperature was raised stepwise from 10 K to 200 K during 90 ns of the corresponding MD run, then kept at 200 K for 90 ns of MD run, then in 35 ns raised up to 309 K, and afterwards kept at 309 K simulated for 95 ns (Fig. 4). The total simulation time was of 310 ns of MD run.

Six of six-stranded flat, parallel beta-sheets 6Abeta 25-35 were used to build the beta-sheet stack (**6x6Abeta 25-35**). The 6x6Abeta 25-35 stack was enriched with chlorine counterions and surrounded by 10 Å layer of explicit water molecules.

The 6x6Abeta 25-35 beta-sheet stack system consisting of 34416 (5580) atoms was subjected for 76 ns of MD simulations. The system was heated stepwise in 31 ns starting from T = 10 K till T= 200 K of MD, then it was kept at 200 K for 22.5 ns, afterwards the system was heated up till 309 K in 0.5 ns. After these preparatory steps production MD simulations were carried out for 21 ns at T=309K 309 K (Fig. 27.-Fig.29.).

## III. RESULTS AND DISCUSSION

The **6Abeta 25-35** system energy, temperature and density protocols are shown in Fig. 4- Fig. 6.

Results of the single sheet MD of 6Abeta 25-35 and 10Abeta 25-35 show the stable  $\beta$ -sheet in the C-terminal part across the  $\beta$ -sheet region from Ile31 to Leu34 (Fig.7- Fig.8, Fig. 10-Fig.11). The  $\beta$ -sheet over the region Ser26-Lys28 is fluctuating with the  $\beta$ -sheet melting time to time. The middle strands 3 - 6 of the six stranded  $\beta$ -sheet also form  $\beta$ -structure across the Ser26-Lys28 region, while the  $\beta$ -structure over the Ser26-Lys28 region is melting at the  $\beta$ -sheet side strands 1-2 and 5-6. Six stranded  $\beta$ -sheet 6Abeta 25-35 is stable at 200 K, but it starts melting with the heating up from the 300K, and it dissolves at 309 K, when the strands accept coil-coil structure with some  $\alpha$ -helical elements (Fig.9, Fig. 12, Fig. 13c).

Analyses of the 6Abeta 25-35  $\beta$ -sheet at 200 K, where the  $\beta$ -sheet is stable, shows that the  $\beta$ -sheet is kept together by backbone hydrogen bonding (Fig.14 - Fig. 15) and by few flickering sidechain hydrogen bonding (Fig. 14), and hydrophobic residues Ile31, Ile32, Leu34, Met35.

During the course of simulation when the system shows the stability of  $\beta$ -sheet, the distances between the mass centers of the adjacent strands of the beta-sheet are about 5 Å (Fig.16 – Fig. 22), which is in concord with NMR data of 5 Å between nearby strands throughout the entire length of the peptide sequence [31, 37].

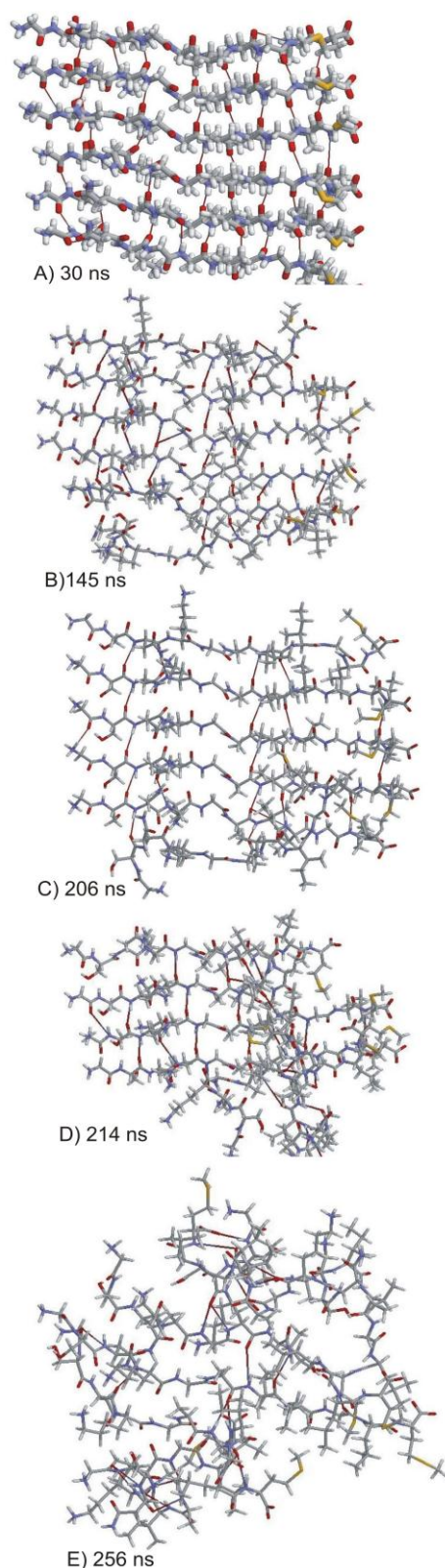


Fig. 15. Hydrogen bonding of 6Abeta 25-35 system  $\beta$ -sheet at a) 30 ns, b) 145 ns, c) 206 ns, d) 214 ns, e) 256 ns of MD run.

Ten stranded **10Abeta 25-35**  $\beta$ -sheet (Fig.23- Fig. 26.) was stable upon heating till 270 K and began to lose the  $\beta$ -structure at 280 K, and it totally dissolved at 290 K, suggesting that for

stabilization the  $\beta$ -sheet neighboring strands are probably not so important than the nearby beta sheets in a protofibril.

The additional four strands in 10Abeta 25-35 comparing to 6Abeta 25-35 do not stabilize the  $\beta$ -sheet.

Both single  $\beta$ -sheets (6Abeta 25-35 and 10Abeta 25-35) tend to cooperate alongside with  $\beta$ -sheets in nearby periodic boxes suggesting that more than 5 Å layer periodic water box is needed to simulate the isolated single  $\beta$ -sheet.

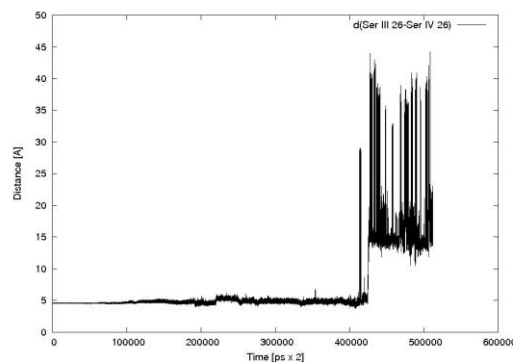


Fig. 16. Mass center distances between Serine 26 (III strand)-Serine 26 (IV strand)

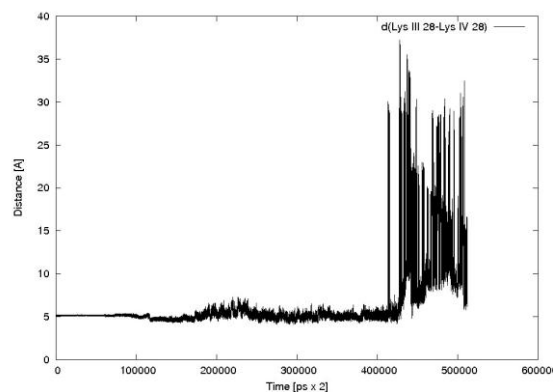


Fig. 17. Mass center distances between Lysine 28 (III strand)-Lysine 28 (IV strand)

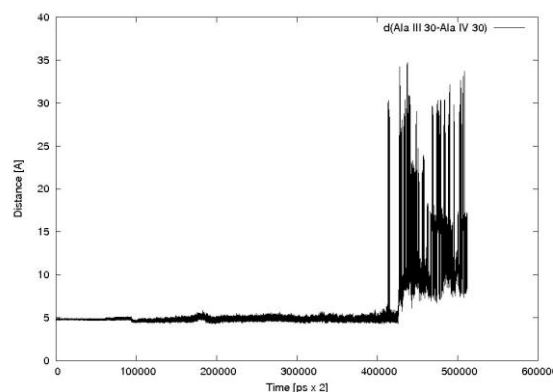


Fig. 18. Mass center distances between Alanine 30 (III strand)-Alanine 30 (IV strand)

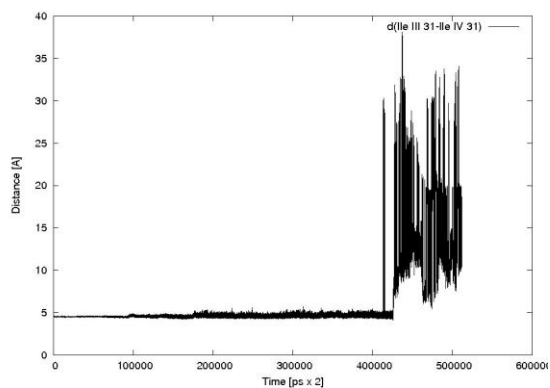


Fig. 19. Mass center distances between Isoleucine 31 (III strand)-Isoleucine 31 (IV strand)

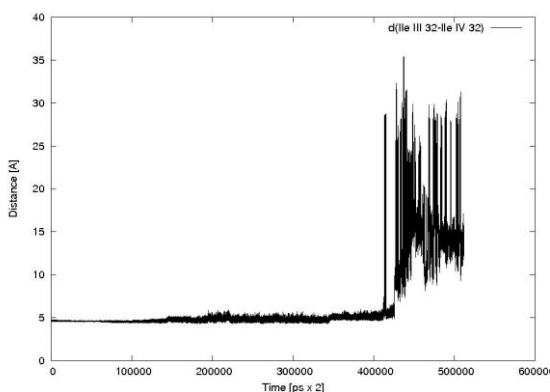


Fig. 20. Mass center distances between Isoleucine 32 (III strand)-Isoleucine 32 (IV strand)

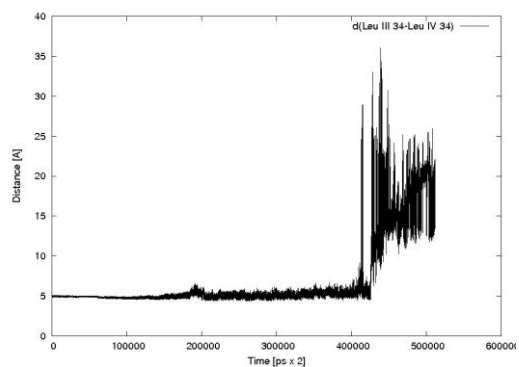


Fig. 21. Mass center distances between Leucine 34 (III strand)-Leucine 34 (IV strand)

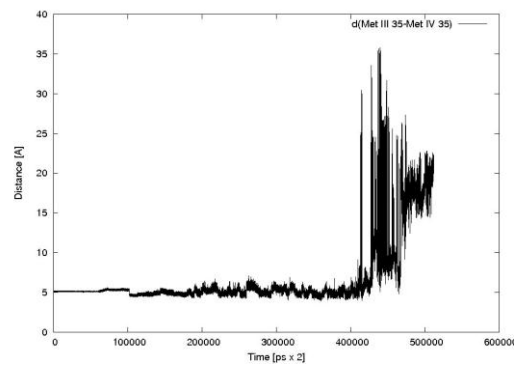


Fig. 22. Mass center distances between Methionine 35 (III strand)-Methionine 35 (IV strand)

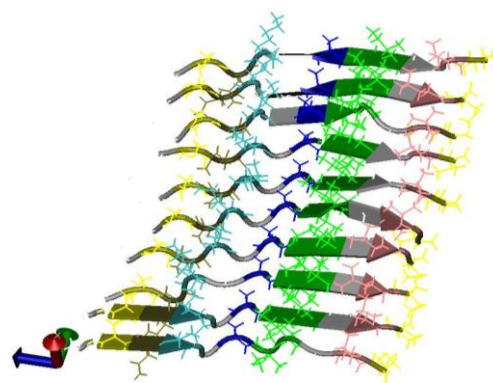


Fig. 23. Front view of 10Abeta 25-35 system after 30ns of MD run

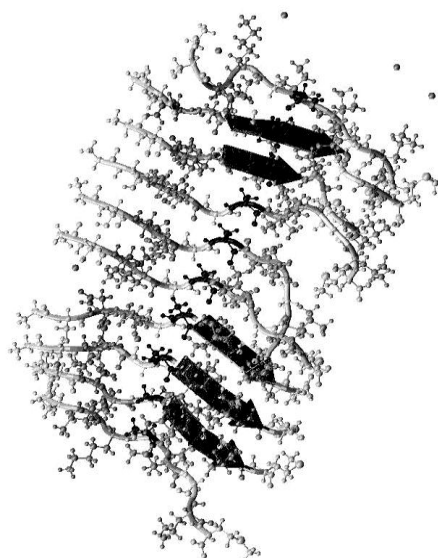


Fig. 24. Front view of 10Abeta 25-35 system after 145ns of MD run

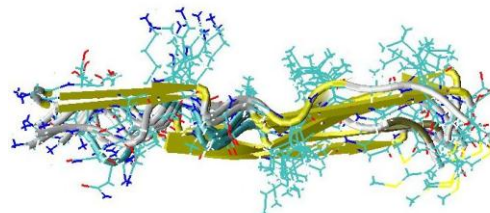


Fig. 25. Side view of 10Abeta 25-35 system after 30ns of MD run

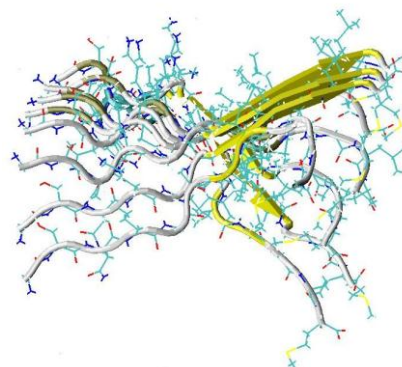


Fig. 26. Side view of 10Abeta 25-35 system after 145ns of MD run

It should be noted that here we simulated the reverse beta-sheet formation: starting from a beta sheet and heating it up until it dissolves. It led to the conclusion that to stabilize the beta sheet against thermal motions, some external factors of surrounding media should be present to shift the conformational equilibrium from coil-coil or  $\alpha$ -helical structures towards extended beta strands, which could willingly form a stable beta-sheet.

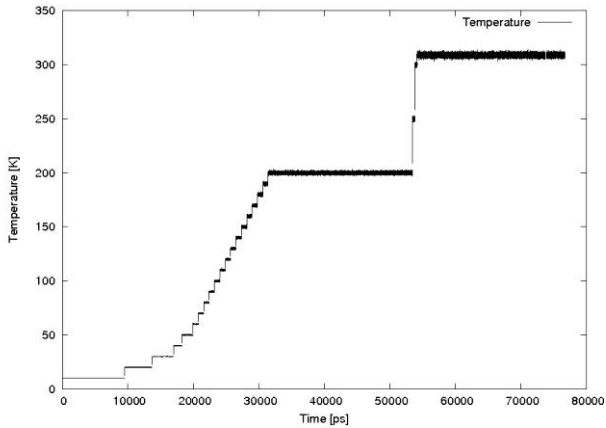


Fig. 27. Temperature over time of the beta sheet stack 6x6Abeta 24-35.

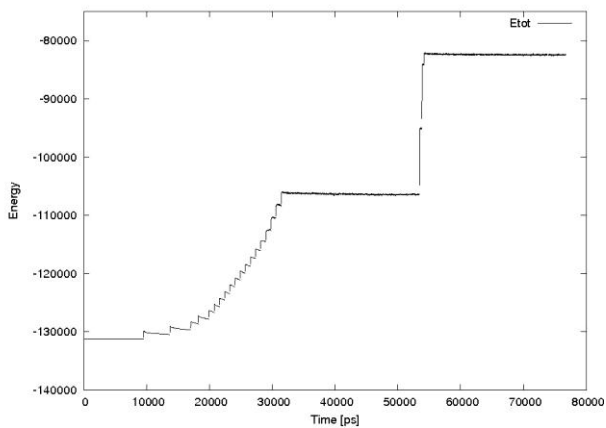


Fig. 28. Energy over time of the beta sheet stack 6x6Abeta 24-35

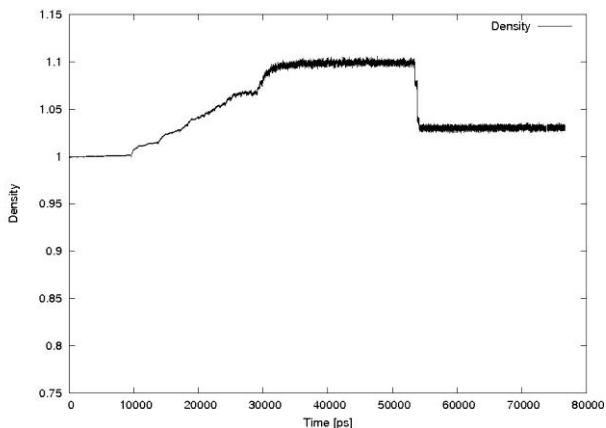


Fig. 29. Density over time of the beta sheet stack 6x6Abeta 24-35

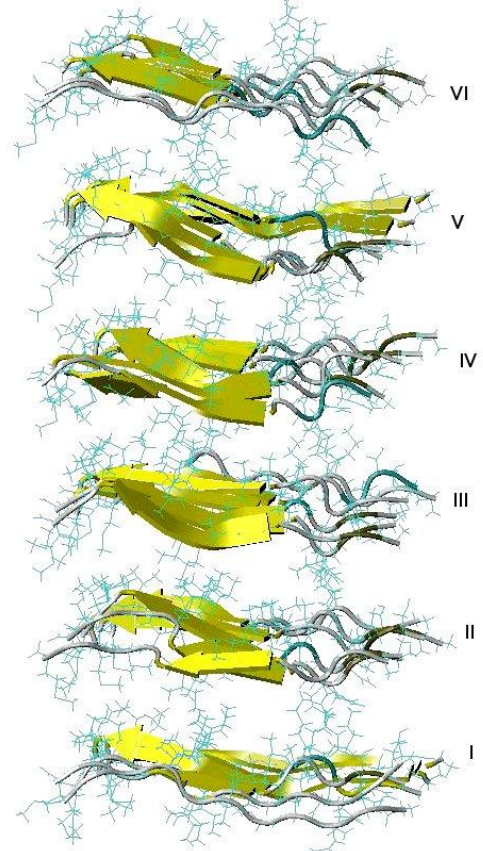


Fig. 30. 6x6Abeta 25-35 system after 4ns of MD run at 10 K

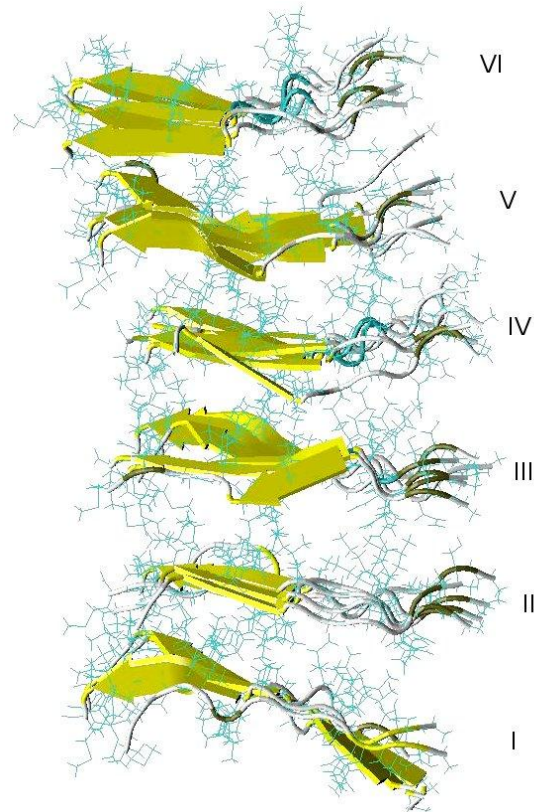


Fig. 31. 6x6Abeta 25-35 system after 36ns of MD run at 200 K

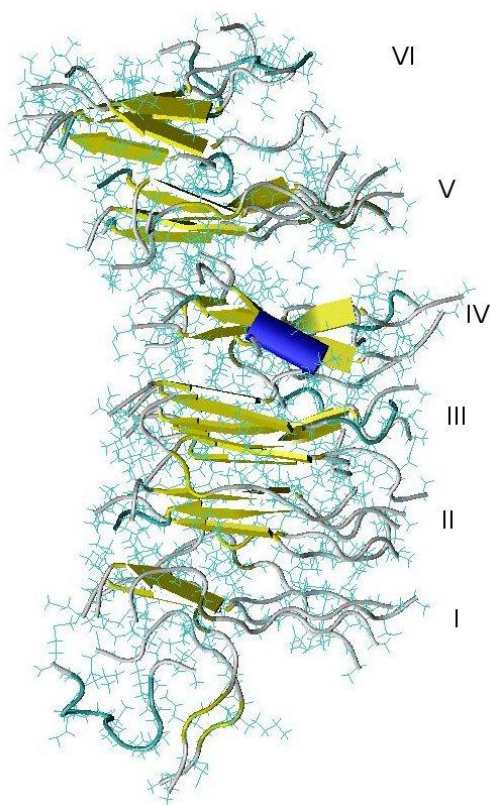


Fig. 32. 6x6Abeta 25-35 system after 58ns of MD run at 309 K

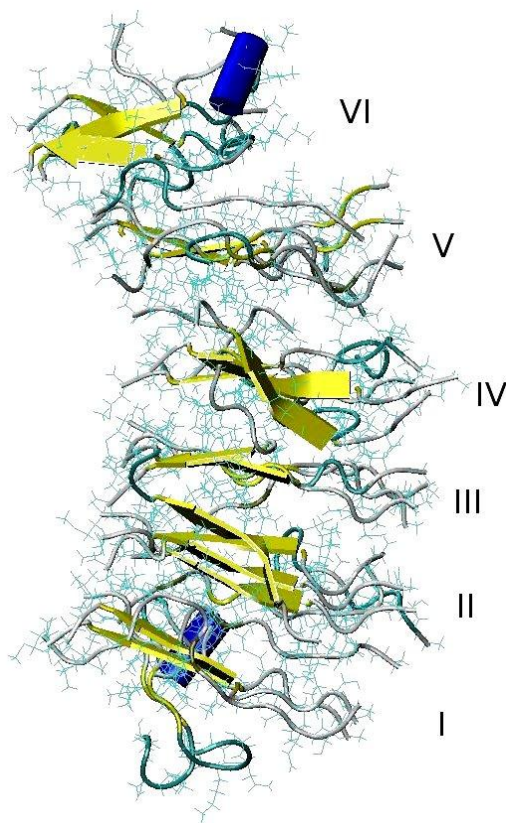


Fig. 33. 6x6Abeta 25-35 system after 76ns of MD run at 309 K

Results of the MD of the multiple  $\beta$ -sheet stack 6x6Abeta 25-35 at 200 K show stable  $\beta$ -sheet structure (from Ile31 – Leu34), and the  $\beta$ -sheet is melting from time to time from Gly25 – Ser26 and Lys28 - Ala30 (Fig. 30-Fig.33). This result is in agreement with the experiments that indicated that the N-terminal part of Abeta 25-35 is more flexible than the C-terminal part [39].

Intra-sheet backbone hydrogen bonding keeps together the  $\beta$ -sheets of the  $\beta$ -sheet stack. Apart from that the system is stabilized by flickering sidechain bonding and by the few inter-sheet hydrogen bonds between the sidechain of Lys28 hydrogen and the backbone carbonyl of Gly29 in the nearby  $\beta$ -sheet.

The strongest intra  $\beta$ -sheet that keeps the stack together comprises the Ile31 and Ile32 residues that form the main part of the hydrophobic core. Apart from that, the  $\beta$ -sheets of the  $\beta$ -sheet stack 6x6Abeta 25-35 are kept together by the hydrophobic interactions of residues Leu34 and Met35 and by the electrostatic interactions of residues Ser25 and Asn27.

During the course of rising temperature from 200K till 309K the 6x6Abeta 25-35  $\beta$ -sheet stack tended to associate with the stack in a nearby periodic box regardless of the presence of a 10Å water layer surrounding the system.

At 309K the  $\beta$ -sheet of the stack 6x6Abeta 25-35 was kept mainly in the C-terminal part of the system over the region Ile31 to Leu34 and from time to time over Ser26-Asn27 in the N-terminal part (Fig. 32-Fig.33).

Apart from forming the  $\beta$ -structure a single strand of Abeta 25-35 stack tends to jump away from the stack and turns from  $\beta$ -structure to coil conformation with the further perspective to turn to  $\alpha$ -helix (Fig. 32- Fig. 33). This is in accordance with literature data suggesting the Abeta 25-35 peptide inhering both  $\beta$ -structure and  $\alpha$ -helical structure in water and membrane environment [38].

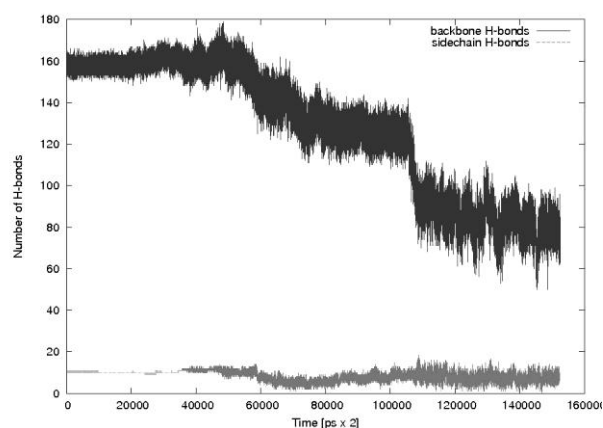


Fig. 34. Hydrogen bonding of 6x6Abeta 25-35  $\beta$ -sheet stack. Number of backbone hydrogen bonds – dark gray, number of sidechain hydrogen bonds – light gray.

#### IV. CONCLUSIONS

Both single  $\beta$ -sheet systems of Abeta 25-35, are kept together by backbone hydrogen bonding. 6Abeta 25-35 and 10Abeta 25-35 systems show the stable  $\beta$ -structure at 200K temperature. 6Abeta 25-35 and 10Abeta 25-35 systems

collapse loosing  $\beta$ -structure at 309K temperature, indicating that the supplementary  $\beta$ -sheets are required for the  $\beta$ -structure stabilization.

Both single  $\beta$ -sheets (6Abeta 25-35 and 10Abeta 25-35) tend to cooperate alongside with the  $\beta$ -sheets in nearby periodic boxes. To examine single  $\beta$ -sheet, more than 5 Å layer periodic water box is needed. The additional four strands in the 10Abeta 25-35  $\beta$ -sheet comparing to the 6Abeta 25-35  $\beta$ -sheet do not stabilize the  $\beta$ -sheet.

Intra-sheet backbone hydrogen bonding keeps together the  $\beta$ -sheets in the  $\beta$ -sheet stack of Abeta 25-35. The strongest intra  $\beta$ -sheet, which keeps the stack together, is comprised of Ile31 and Ile32 forming the main part of the hydrophobic core. Apart from that, in the Abeta 25-35  $\beta$ -sheet stack the  $\beta$ -sheets are kept together by Leu34 and Met35 hydrophobic interactions and Ser25 and Asn27 electrostatic interactions. In several cases the sidechain of Lys28 makes hydrogen bonding with the backbone carbonyl of Gly29 in the nearby  $\beta$ -sheet. The C-terminal part of the  $\beta$ -sheet stack is more prone to keep the  $\beta$ -sheet structure while the N-terminal part of the  $\beta$ -sheet stack is more flexible which is in accord with the experimental data [39].

A single strand of the Abeta 25-35  $\beta$ -sheet stack tends to jump away from the stack and turns from  $\beta$ -structure to coil conformation with the further perspective to turn to  $\alpha$ -helix. This is in accordance with literature data suggesting that the Abeta 25-35 peptide depending on conditions could form both  $\beta$ -structure and  $\alpha$ -helical structure in water and membrane environment [38].

#### ACKNOWLEDGMENTS

This work was supported by European Economic Area block grant "Academic Research" LV0015.EEZ09AP - 68 "Molecular modelling of amyloid formation". Calculations were performed on computers of the Gdansk Academic Computer Center TASK.

Some calculations were done with Program MOE [40].

The Figures were prepared by VMD [41], RASMOL [42].

#### REFERENCES

1. Stefani, M., Dobson, C. M. Protein aggregation and aggregate toxicity: new insights into protein folding, misfolding diseases and biological evolution. *Journal of Molecular Medicine*, 2003, vol. 81, p. 678-699.
2. Khurana, R., R., Ionescu-Zanetti, C., Pope, M., Li, J., Nielson, L., Ramirez-Alvarado, M., Regan, L., Fink A. L., Cartery, S. A. A general model for amyloid fibril assembly based on morphological studies using atomic force microscopy. *Biophysical Journal*, 2003, vol. 85, p. 1135-1444.
3. Cohen, A. S., Jones, L. A. Amyloid and amyloidosis. *Current Opinion in Rheumatology*, 1991, vol. 4, p. 9405.
4. Rochet, J. C., Conway, K. A., Lansbury, P. T., Jr. Inhibition of fibrillization and accumulation of prefibrillar oligomers in mixtures of human and mouse alpha-synuclein. *Biochemistry*, 2000, vol. 39, p. 10619-10626.
5. Dobson, C. M. Protein folding and disease: a view from the first Horizon Symposium. *Nature Reviews Drug Discovery*, 2003, vol. 2, p. 154-160.
6. Lee, J. P., Stimson, E. R., Ghilardi, J. R., Mantyh, P. W., Lu, Y. A., Felix, A. M., Llanos, W., Behbin, A., Cummings, M., Van Crielinge, M., et al. 1H NMR of A<sub>β</sub> amyloid peptide congeners in water solution. Conformational changes correlate with plaque competence. *Biochemistry*, 1995, vol. 34, p. 5191-5200.
7. Selkoe, D. J. Cell biology of protein misfolding: the examples of Alzheimer's and Parkinson's diseases. *Nature Cell Biology*, 2004, vol. 6, p. 1054-1061.
8. Lei, H. *Protein & Cell*, 2010, vol. 1, Nr. 4, p. 312-314.
9. Chini M. G., Scrima M., D'Ursi A. M., Bifulco G. Fibril aggregation inhibitory activity of the beta sheet breaker peptides: a molecular docking approach, *Journal of Peptide Science*, 2009, vol. 15, p. 229-234.
10. Sarroukh R., Cerf E., Derclaye S., Yves F., Dufrene F., Goormaghtigh, E., Ruyschaert J. M., Raussens V. Transformation of amyloid b(1-40) oligomers into fibrils is characterized by a major change in secondary structure. *Cellular and Molecular Life Sciences*, Springer Basel AG 2010.
11. Campiglia, P., Esposito, C., Scrima, M., Gomez-Monterrey, I., Bertamino, A., Grieco, P., Novellino, E., D'Ursi, A. M. Conformational Stability of Ab-(25-35) in the Presence of Thiazolidine Derivatives. *Chemical Biology & Drug Design*, 2007, vol. 69, p. 111-118.
12. Selkoe, D. J. Translating cell biology into therapeutic advances in Alzheimer's disease. *Nature*, 1999, 399, p. A23-A31.
13. Seubert, P., Vigo-Pelfrey, C., Esch, F., Lee, M., Dovey, H., Davis, D., Sinha, S., Schlossmacher, M. G., Whaley, J., Swindlehurst, C., McCormack, R., Wolfert, R., Selkoe, D. J., Lieberburg, I., Schenk, D. Isolation and quantification of soluble Alzheimer's b-peptide from biological fluids. *Nature*, 1992, vol. 359, p. 325-327.
14. Barrow, C. J., Zagorski, M. G. Solution structures of beta peptide and its constituent fragments: relation to amyloid deposition. *Science*, 1991, vol. 253, p. 179-182.
15. Martins, I. C., Kuperstein, I., Wilkinson, H., Maes, E., Vanbrabant, M., Jonckheere, W., Van Gelder, P., Hartmann, D., D'Hooge, R., De Strooper, B., Schymkowitz, J., Rousseau, F. Lipids revert inert Abeta amyloid fibrils to neurotoxic protofibrils that affect learning in mice. *The EMBO Journal*, 2008, vol. 27, Nr. 1, p. 224-233.
16. Walsh, D. M., Hartley, D. M., Kusumoto, Y., Fezoui, Y., Condron, M. M., Lomakin, A., Benedek, G. B., Selkoe, D. J., Teplow, D. B. Amyloid beta-protein fibrillogenesis. Structure and biological activity of protofibrillar intermediates. *The Journal of Biological Chemistry*, 1999, vol. 274, p. 25945-25952.
17. Hardy, J., Selkoe, D. J. The amyloid hypothesis of Alzheimer's disease: progress and problems on the road to therapeutics. *Science*, 2002, vol. 297, p. 353-356.
18. Harper, J. D., Wong, S. S., Lieber, C. M., Lansbury P. T. Assembly of A beta amyloid protofibrils: an in vitro model for a possible early event in Alzheimer's disease. *Biochemistry*, 1999, vol. 38, p. 8972-8980.
19. Lashuel H. A., Hartley D, Petre B. M, Walz T, Lansbury P. T. Neurodegenerative disease: Amyloid pores from pathogenic mutations. *Nature*, 2002, vol. 418, p. 291.
20. Bitan, G., Lomakin A., Teplow, D. B. Amyloid- $\beta$ -protein oligomerization: prenucleation interactions revealed by photo-induced cross-linking of unmodified proteins. *Journal of Biological Chemistry*, 2001, vol. 276, p. 35176-35184.
21. Collins, S. R., Dougllass, A., Vale, R. D., Weissman, J. S. Mechanism of prion propagation: amyloid growth occurs by monomer addition, *PLoS Biology*, 2004, vol. 2, p. 1582-1590.
22. Lashuel, H. A., Lansbury, P. T., Jr., Are amyloid diseases caused by protein aggregates that mimic bacterial pore-forming toxins. *Quarterly Reviews of Biophysics*, In: Cambridge University Press, Cambridge, UK, 2006, p. 167-201.
23. Gavin Tsai, H. H., Lee, J. B., Tseng, S. S., Pan, X. A., Shih, Y. C. Folding and membrane insertion of amyloid-beta (25-35) peptide and its mutants: Implications for aggregation and neurotoxicity. *Proteins: Structure, Function and Bioinformatics*, 2010, vol. 78, p. 1909-1925.
24. Lin, M. C. A., Kagan, B. L. Electrophysiologic properties of channels induced by A beta 25-35 in planar lipid bilayers. *Peptides* 2002, vol. 23, p. 1215-1228.
25. Kagan, B. L., Hirakura, Y., Azimov, R., Azimova, R., Lin, M. C. The channel hypothesis of Alzheimer's disease: current status. *Peptides* 2002, vol. 23, p. 1311-1315.
26. Quist, A., Doudevski, I., Lin, H., Azimova, R., Ng, D., Frangione, B., Kagan, B., Ghiso, J., Lal, R. Amyloid ion channels: a common structural link for protein-misfolding disease, *Proceedings of the National Academy of Sciences, USA* 2005, vol. 102, p. 10427-432.

27. **Pike C. J., Burdick D., Walencewicz A. J., Glabe C. G., Cotman C. W.** Neurodegeneration induced by b-amyloid peptide in vitro: the role of peptide assembly state. *The Journal of Neuroscience*, 1993, vol. 16, p. 1676-687.
28. **Pike C. J., Walencewicz-Wasserman A. J., Kosmoski J., Cribbs D. H., Glabe C. G., Cotman C. W.** Structure-activity analyses of b-amyloid peptides: contributions of the b 255 region to aggregation and neurotoxicity. *Journal of Neurochemistry*, 1995, vol. 64, p. 253-65.
29. **Terzi E., Holzemann G., Seelig J.** Alzheimer b-amyloid peptide 255: electrostatic interactions with phospholipid membranes. *Biochemistry*, 1994, vol. 33, p. 7434-441.
30. **Soto C., Castano E. M., Frangione B., Inestrosa N. C.** The alpha-helical to beta-strand transition in the amino-terminal fragment of the Amyloid beta-peptide modulates amyloid formation, *Journal of Biological Chemistry*, 1995, vol. 270, Nr. 7.
31. **Benzinger, T. L., Gregory, D. M., Burkoth, T. S., Miller-Auer, H., Lynn, D. G., Botto, R. E. Meredith, S. C.** Two-dimensional structure of beta-amyloid(105) fibrils. *Biochemistry*, 2000, vol. 39, p. 3491-3499.
32. **D'Ursi A. M., Armenante M. R., Guerrini R., Salvadori S., Sorrentino G., Picone D.** Solution Structure of Amyloid beta-peptide (25-35) in different media, *Journal of Medicinal Chemistry*, 2004, vol. 47, p. 4231-4238.
33. **Pearlman, D. A., Case, D. A., Caldwell, J. W., Ross, W. S., Cheatham, T. E. III, DeBolt, S., Ferguson, D., Seibel, G., Kollman, P.** AMBER, a package of computer programs for applying molecular mechanics, normal mode analysis, molecular dynamics and free energy calculations to simulate the structural and energetic properties of molecules. *Computer Physics Communications*, 1995, vol. 91, p. 1-41.
34. **Case, D. A., Cheatham, T., Darden, T., Gohlke, H., Luo, R., Merz, K. M. Jr., Onufriev, A., Simmerling, C., Wang, B., Woods, R.** The Amber biomolecular simulation programs. *Journal of Computational Chemistry*, 2005, vol. 26, p. 1668-1688.
35. **Ponder, J. W., Case, D. A.** Force fields for protein simulations. *Advances in Protein Chemistry*, 2003, vol. 66, p. 27-85.
36. **Antzutkin, O. N., Balbach, J. J., Leapman, R. D., Rizzo, N. W., Reed, J., Tycko, R.** Multiple quantum solid-state NMR indicates a parallel, not antiparallel, organization of b-sheets in Alzheimer's b-amyloid fibrils. *Proceedings of the National Academy of Sciences, USA*, 2000, vol. 97, p. 13045-13050.
37. **Balbach, J. J., Petkova, A. T., Oyler, N. A., Antzutkin, O. N., Gordon, D. J., Meredith, S. C., Tycko, R.** Supramolecular Structure in Full-Length Alzheimer's b-Amyloid Fibrils: Evidence for a Parallel b-Sheet Organization from Solid-State Nuclear Magnetic Resonance. *Biophysical Journal*, 2002, vol. 83, p. 1205-1216.
38. **Di Carlo M.** Beta amyloid peptide: from different aggregation forms to the activation of different biochemical pathways. *European Biophysics Journal*, 2010, vol. 39, p. 877-888.
39. **Kohno, T., Kobayashi, K., Maeda, T., Sato, K., Takashima, A.** Three-dimensional structures of the amyloid beta peptide (25-35) in membrane mimicking environment. *Biochemistry*, 1996, vol. 35, p. 16094-16104.
40. **Chemical Computing Group C., Molecular Operative Environment (MOE) 2008.** Available: <http://www.chemcomp.com/>
41. **Humphrey, W., Dalke, A. Schulten, K.** "VMD - Visual Molecular Dynamics" *J. Molec. Graphics*, 1996, v. 14, p. 33-38.
42. **Roger, S., Milner-White, E. J.** "RasMol: Biomolecular graphics for all", *Trends in Biochemical Sciences*, 1995, vol. 20, Nr. 9, p. 374.
- Vita Duka** obtained Bsc. math. in 2009 at the Faculty of Physics and Mathematics of the University of Latvia. She is taking Masters degree in mathematics at the University of Latvia and since 2010 is a research assistant at the Latvian University of Agriculture. European Economic Area grant EEZ-068 "Molecular modelling of amyloid formation" executive, 2009 - 2010. Member of the Latvian Mathematical Society (LMB)
- Isabella Bestel** obtained Dr. Sci. in Medicinal Chemistry in 1998 at the University of Paris XI Associate professor in medicinal chemistry at the University of Paris XI from 1998 to 2006, and at the Bordeaux 2 University since 2006. Researcher in the Pharmaceutical Laboratory Servier in 1998. Research interests: Molecular modeling of proteins and ligand-protein interactions, design and synthesis of organic molecules targeting Alzheimer's disease and able to inhibit A-beta amyloid aggregation, vectorization of drugs based on amphiphilic molecules. Member of the Therapeutic Chemical Society.
- Cezary Czaplewski** obtained Dr.Sc.Chemistry in 1998 at the University of Gdansk (Poland). Associate Professor at the Faculty of Chemistry, University of Gdansk, visiting Scientist at the Korea Institute for Advanced Study, at John von Neumann Institute for Computing, Juelich, Germany and at Cornell Cornell University, Ithaca, NY, USA. Research interests: Computer simulations of structure and dynamics of polymers and biopolymers, hydrophobic interactions, development and applications of various methods of computational chemistry (global optimization, molecular dynamics, Monte Carlo, replica exchange, coarse-grained force fields). Member of European Peptide Society and of the European Distance and E-Learning Network.
- Adam Liwo** obtained Dr. Sci. in Theoretical Chemistry at the University of Gdansk in 1997. Full Professor and Head of the Group of Molecular Modeling at the Faculty of Chemistry, University of Gdansk, Poland; Senior Research Associate, Faculty of Chemistry, Baker Laboratory of Chemistry and Chemical Biology, Cornell University, Ithaca, NY, USA (2003-2010). Research interests: statistical mechanics of complex systems, design of empirical force fields, protein folding, numerical algorithms in chemistry, member of the American Chemical Society, Biophysical Society, Polish Bioinformatics Society, Polish Society of Computer Simulation, Scientific Society of Gdansk
- Inta Liepina** obtained PhD at the University of Gdansk, Poland, in 2003. Is a molecular modeler and lead researcher at the Latvian Institute of Organic Synthesis. Manager of the European Economic Area project EEZ-68 "Molecular modelling of amyloid formation". Visiting scientist at the Friedrich Schiller University of Jena, Germany, (1993, 1995-1996), Visiting Scientist at the University of Gdansk, Poland, (1998-2007), Visiting Scientist at the University of Helsinki Finland (2007-2009), Visiting Scientist at the University of Bordeaux II. (2008-2009). Research interests: molecular modeling of amyloids, gene transfection agents, proteins, receptor and ligand interactions. Member of European Peptide Society, World Organization of Theoretically Oriented Chemists (WATOC), Latvian Mathematical Society, Latvian Biochemical Society (member of FEBS).

### Vita Duka, Isabella Bestel, Cezary Czaplewski, Adam Liwo, Inta Liepiņa. Amiloīda beta proteīna 25-35 beta-sloksnes un beta-slokšņu grēdas molekulārā modelēšana

Amiloidoze ir šķīstošu proteīnu atlocīšanās, nepareiza salocīšanās un pašasambļēšanās nešķīstošās fibrillās, kas aizvieto funkcionējošas šūnas vai bloķē starpšūnu savienojumus. Amiloidozes veidošanās mehānisms vēl nav skaidrs. β-amiloīda proteīns (Abeta) 1- 42 rada cilvēku amiloidozi, kas izsauc Alcheimera slimību. Šis darbs pēta β-amiloīda proteīna 25-35 (Abeta 25-35), GSNKGAIIGLM, β-struktūras veidošanos. Plakana, paralēla sešu virkņu β-sloksne (6Abeta 25-35) un desmit virkņu β-sloksne (10Abeta 25-35), kā arī β-slokšņu grēda, kas konstruēta no sešām 6Abeta 25-35 β-sloksnēm (6x6Abeta 25-35), tika simulētas ar molekulāro dinamiku (MD) atbilstoši 210 ns, 310 ns un 76 ns, lietojot programmu paketi Amber 9.0 ar spēku lauku f99. Temperatūra tika celta pakāpienveidīgi no 10 K līdz 309 K, ar ilgākiem konstantas temperatūras intervāliem pie 200 K un 309 K.

6Abeta 25-35 un 10Abeta 25-35 atsevišķu β-slokšņu sistēmas parādīja stabili β-struktūru pie 200 K temperatūras, bet tās kolapsēja, zaudējot β-struktūru pie 309 K temperatūras, liekot secināt, ka papildus β-sloksnes nepieciešamas β-struktūras stabilizēšanai. Četras papildus peptīdu virknes 10Abeta 25-35 β-sloksnē, salīdzinot ar 6Abeta 25-35, nestabilizē β-sloksni.

$\beta$ -Slokšņu grēdā 6x6Abeta 25-35 stiprākā starpslokšņu salipšana notiek ar rezidiju Ile31 un Ile32 veidoto hidrofobo serdi. Bez tam  $\beta$ -slokšņu grēdu kopā tur rezidiju Leu34 un Met35 hidrofobās mijiedarbības un rezidiju Ser26 un Asn27 elektrostatiskā mijiedarbības. Dažos gadījumos rezidija Lys28 sānu ķēde veido ūdeņraža saiti ar blakus  $\beta$ -slokšnes Gly29 pamatķēdes karbonilgrupu.  $\beta$ -Slokšņu grēdas C-gala pusei ir lielāka tieksme saglabāt  $\beta$ -slokšņu struktūru, bet  $\beta$ -slokšņu grēdas N-gala puse ir lokanāka; kas ir saskaņā ar eksperimentāliem datiem [39]. Atsevišķs peptīdu virknes no Abeta 25-35 grēdas cenšas atdalīties un pāriet no  $\beta$ -struktūras spirālveida konformācijā ar tālāku perspektīvu pāriet  $\alpha$ -spirālē. Tas ir saskaņā ar literatūras datiem, kas norāda, ka Abeta 25-35 peptīds atkarībā no ārējiem apstākļiem var veidot gan  $\beta$ -struktūru, gan  $\alpha$ -spirāles struktūru ūdenī un membrānā [38].

**Вита Дука, Изабелла Бестел, Цезарь Цаплевски, Адам Ливо, Инта Лиениня. Молекулярное моделирование одного бета-листа и стека из бета-листов белка бета-амилоид 25 - 35**

Амилоидоз – это неправильное свёртывание и агрегация самособирающихся, растворимых белков в нерастворимых волокнах, которые заменяют функциональные клетки или блокирует связь между ними. Механизм формирования амилоидов до сих пор неясен. Белок бета-амилоид 1-42 несёт ответственность за формирование человеческого амилоидоза, это приводит к болезни Альцгеймера. В работе изучается образование  $\beta$ -структуры амилоида на фрагменте белка амилоид бета 25-35 (Abeta 25-35), GSNKGAIIGLM. Плоские, параллельные бета-листы из шести нитей (6Abeta 25-35) и из десяти нитей (10Abeta 25-35), а также стек из шести бета-листов 6Abeta 25-35 (6x6Abeta 25-35) 210ns, 310ns и 76ns моделировались молекулярной динамикой (МД), используя программу Amber 9.0 и силовое поле f99. Температура поднималась ступенчато от 10К до 200К, выдерживая некоторое время, и ступенчато поднималась от 200К до 309 К, также выдерживая некоторое время.

6Abeta 25-35 и 10Abeta 25-35 системы одного бета-листа, показывают стабильную  $\beta$ -структуру при температуре 200К, но теряют  $\beta$ -структуру при температуре 309К, указав, что дополнительные  $\beta$ -листы необходимы для стабилизации  $\beta$ -структуры. Дополнительные четыре нити в 10Abeta 25-35 (по сравнению с 25-35 6Abeta) не стабилизируют  $\beta$ -лист.

В бета-листе стека 6x6Abeta 25-35 сильнейшее склеивание внутри  $\beta$ -листов осуществляется от Ile31 до Ile32, формируя основную часть гидрофобного ядра. Кроме того, в  $\beta$ -лист стека 6x6Abeta 25-35  $\beta$ -листы держатся вместе, благодаря гидрофобным взаимодействиям от Leu34 до Met35 и электростатическим взаимодействиям от Ser25 до Asn27. В ряде случаев боковые цепи из Lys28 создают водородные связи с кислородом из основной цепи Gly29 в близлежащих  $\beta$ -листов. С-концевая часть  $\beta$ -лист стека более склонна сохранить  $\beta$ -лист структуру в то время, как N-концевая часть  $\beta$ -лист стека является более гибкой, что в согласии с экспериментальными данными [39]. Одна нитка Abeta 25-35 от стека стремится в дальнейшей перспективе перейти от  $\beta$ -структуры и превращается в конформацию  $\alpha$ -спираль. Это в соответствии с литературными данными предполагается, что Abeta 25-35 пептид в зависимости от условий может стать как  $\beta$ -структурой, так и  $\alpha$ -спиральной структурой в воде или на мембране [38].